ATOMIC TRANSIT AND DELAYED IONIZATION EFFECTS ON CESIUM BEAM FREQUENCY STANDARDS

Bernardo Jaduszliwer
Chemistry and Physics Laboratory
The Aerospace Corporation
P. O. Box 92957, Los Angeles, CA 90009

ABSTRACT

In a compact cesium beam atomic clock the magnets that perform state selection and analysis transmit a narrow velocity distribution. Increasing the width of the transmitted velocity distribution will increase the beam intensity, but it will also distort the atomic beam amplitude modulation which gives the clock error signal. Detection is accomplished by surface ionization on a hot wire, which acts as a low-pass filter. The combined effects of these processes on the clock's error signal are analyzed in detail for a test case involving an atomic beam which has been square-wave amplitude-modulated by its interaction with the frequency-modulated microwave field. Our analysis, performed for the type of cesium beam tube used on GPS satellites, shows the importance of processes taking place after the atom-microwave interaction is completed for the optimization of the clock's performance.

I. INTRODUCTION

In compact cesium beam atomic clocks, the atomic beam is detected by surface ionization on a hot wire, and hyperfine state preparation and analysis are accomplished by atomic deflection in strongly inhomogeneous magnetic fields. Since atomic deflection in a magnetic field gradient is velocity dependent, only atoms within a relatively narrow range of speeds will follow trajectories leading from the cesium oven to the detector. Two independent processes will smear out the time-dependent (AC) component of the atomic beam signal introduced by microwave frequency modulation. Atoms leaving the microwave interrogation volume simultaneously with different speeds will arrive at the ionizer at different times; the spread in arrival times Δt_A will be determined by the atomic beam velocity spread Δv. Also, atoms arriving at the ionizer simultaneously will leave as ions with an exponential distribution of residence times characterized by a temperature and material dependent ionic dwell time τ. These two processes will introduce a significant smearing of the AC component of the atomic beam signal if either one (or both) of Δt_A and τ are comparable to $T_m/2\pi$, where $T_m = 1/\nu_m$ is the modulation period. The relative importance of these two processes will be determined by the relative length of Δt_A and τ.

The discriminator function of the atomic system is determined primarily by the atomic resonance lineshape and the microwave modulation scheme, since they will determine how microwave detuning is translated into intensity modulation of the atomic beam. But the intensity modulation impressed upon the atomic beam by microwave interrogation will be degraded during transit and detection by the aforementioned processes, thus degrading the discriminator function. The choice of modulation frequency for best clock performance will then not only depend on the atomic resonance lineshape, but also on the atomic velocity distribution and the ionizer time constant.

We have modelled the effects of the smearing of the aforementioned processes for a test case in which the intensity of the state-selected atomic beam incident on the detector is square-wave amplitude modulated:

$$I(t) = I_o \qquad nT_m \le t < (n+1/2)\ T_m \tag{1a}$$

$$I(t) = I_o(1-d) \qquad (n+1/2)\ T_m \le t < (n+1)\ T_m \tag{1b}$$

where n is any integer and d the depth of amplitude modulation ($0 \le d \le 1$). The average atomic beam intensity is given by $\langle I \rangle = I_o\ (d-1/2)$. The depth of amplitude modulation d will in general depend on the microwave detuning, the depth of frequency modulation and the atomic transition lineshape. In some instances we will be taking d = 1 for clarity. This is unrealistic, but does not entail a loss of generality, since the results of our modelling scale linearly with d.

The atomic beam intensity incident on the detector will be given by I'(t), and I_+ (t) will be the ion current (ions/second) emerging off the ionizer surface. If I(t) is periodic of period T_m, so will be I'(t) and $I_+(t)$. Also, $\langle I_+ \rangle = \varepsilon \langle I' \rangle = \varepsilon \langle I \rangle$, where ε is the hot wire ionization efficiency.

We will assume that the AC component of the ion signal is detected by a phase sensitive technique, using as reference a square wave of the same frequency as the modulation. The magnitude of the error signal will be proportional to

$$|E| = \frac{1}{T_m} \int_o^{T_m} |I_+(t) - \langle I_+ \rangle| dt. \tag{2}$$

and it's sign will depend on whether $I_+(t)$ and the reference are in phase or in phase opposition.

II. IONIZER EFFECTS

I_+ can be expressed as $I_+ = \gamma N_+$ where N_+ is the total number of cesium ions on the ionizer surface, and γ the ionic evaporation probability per unit time. The dwell time of the adsorbed ions is given by $\tau = 1/\gamma$, and Hughes and Levinstein [1] have shown that the temperature dependence of τ is given by

$$\tau = \tau_\infty \exp\ (Q_+/kT) \tag{3}$$

where Q_+ is the ionic heat of desorption. Nazarov [2] studied atomic and ionic desorption dynamics for the cesium-tungsten system, and from his work $\tau_\infty \cong 7.9 \times 10^{-12}$ s; $Q_+ \cong 1.84$ eV. Fig. 1 shows τ vs. temperature for cesium ions on a tungsten surface, calculated using Eq. 3 with Nazarov's results. For our test case, we are assuming a tungsten ionizer operated at T ≈ 1220 K, yielding $\tau \cong 3 \times 10^{-4}$s. If I'(t) is the atomic current impinging on the ionizer, the ion current satisfies

$$\tau \frac{dI_+}{dt} + I_+ = \varepsilon I'(t), \tag{4}$$

where typically $\varepsilon \cong 1$.

We will first solve Eq. 4 for two special cases, the intensity of the atomic beam incident on the detector being sine-wave or square-wave

modulated. The first one is of interest because it yields a simple model for the behavior of the ionizer in the frequency domain, while the second one describes our test case when the atomic beam is single-velocity.

If the atomic beam current incident on the ionizer is sine-wave modulated with depth of amplitude modulation d', the solution to Eq. 4 is

$$I_+(t) = \varepsilon I_o\,(1-d'/2) + \frac{\varepsilon I_o'\, d'/2}{(1+4\pi^2\nu_m^2\tau^2)^{1/2}} \cos\,(2\pi\nu_m t-\theta) \qquad (5)$$

where θ = arc tan $2\pi\nu_m\tau$. This shows that in the frequency domain, the ionizer behaves as a simple low pass filter of cutoff frequency $\nu_{co} = 1/2\pi\tau$; the depth of amplitude modulation in the ion signal is given by

$$d_+ = d'/(1+4\pi^2\nu_m^2\tau^2)^{1/2}. \qquad (6)$$

When the atomic beam current incident on the ionizer is square-wave modulated, as described by Eqs. 1a, b, the solution to Eq. 4 is

$$I_+(t) = \varepsilon I_o' \left\{1-d' \Xi \exp\left[-\frac{t - nT_m}{\tau}\right]\right\} \qquad nT_m \le t < (n+1/2)T_m \qquad (7a)$$

$$I_+(t) = \varepsilon I_o' \left\{1-d'+ d' \Xi \exp\left[-\frac{t-(n+1/2)T_m}{\tau}\right]\right\} \qquad (n+1/2)T_m \le t < (n+1)T_m \qquad (7b)$$

where $\Xi = [1 + \exp(-T_m/2\tau)]^{-1}$. The depth of amplitude modulation in the ion signal is given now by

$$d_+ = \frac{1- \exp(-1/2\ \nu_m\tau)}{1 + \exp(-1/2\nu_m\tau)}\, d'. \qquad (8)$$

Eqs. 6 and 8 show clearly the role of the ionic dwell time τ on the degradation of the AC component of the signal, as illustrated in Fig. 2. A general solution to Eq. 4 can be obtained using the Green's function for the problem, G(t,t'), given by

$$G(t,t') = 0 \qquad t < t' \qquad (9a)$$

$$G(t,t') = \frac{1}{\tau} \exp\,[-(t-t')/\tau] \qquad t \ge t' \qquad (9b)$$

and then, for an arbitrary atomic beam incident on the detector,

$$I_+(t) = \frac{e^{-t/\tau}}{\tau} \int_{-\infty}^{t} e^{t'/\tau}\, I'(t')\, dt'. \qquad (10)$$

III. WAVEFORM DISTORTION

Audoin et al. [3] have discussed the effects of the atomic velocity distribution on the frequency stability of optically pumped, optically detected cesium beam frequency standards. Similar effects must be incorporated into our analysis of waveform distortion effects in compact cesium beam tubes.

Let $dN_v = I(t')\, g(v)dv$ be the number of atoms with speeds between v and v+dv in the amplitude-modulated beam passing per unit time through a given cross section of the tube of trajectories leading to the ionizer. The state selecting and analyzing magnets transmit a normalized atomic beam speed distribution $g(v)$. The same atoms will arrive at the detector at time $t = t' + \bar{t}_A (\bar{v}/v)$, where $\bar{v}$ and $\bar{t}_A$ are the average atomic speed and transit time, respectively. The atomic beam current impinging on the ionizer at time t will be given by

$$I'(t) = \int_0^\infty I(t-\bar{t}_A\bar{v}/v)\, g(v)\, dv. \qquad (11)$$

This result can be inserted in Eq. 10 to obtain the ion current out of the ionizer. If we assume phase-sensitive detection with a properly phased square wave reference signal, the magnitude of the corresponding error signal can be calculated using Eq. 2.

We have used the above procedure for our test case atomic beam, with initial square wave intensity modulation as given by Eqs. 1a,b. We assume the velocity distribution to be Gaussian, of average $\bar{v}$ and standard deviation σ.

Numerical integration of Eqs. 11 and 10 yields the waveforms into and out of the ionizer. Fig. 3 presents the results for the following parameters: $\nu_m = 440$ Hz, $d = 1$, $\bar{t}_A = 1.4 \times 10^{-2}$ s, $\bar{v} = 114$ m/s, $\sigma = 10$ m/s, $\varepsilon = 1$ and $\tau = 3 \times 10^{-4}$ s. It shows that in this case the distortion of the ion current waveform is dominated by the exponential character of the ionizer emission. Fig. 4 shows the corresponding waveforms for $\sigma = 30$ m/s, all other parameters being the same. In this case, velocity spread effects dominate waveform distortion.

Once the ion current waveform has been determined, Eq. 2 can be used to calculate the detected error signal. Fig. 5 shows that for the set of parameters described above, the magnitude of the relative error signal, $|E|/I_o$, is quite insensitive to the atomic beam velocity spread for very narrow speed distributions ($\sigma \leq 4$ m/s), but as the velocity spread increases, $|E|/I_o$ decreases steadily.

IV. INTENSITY EFFECTS

The clock's error signal will be proportional to (E/I_o), the relative error signal discussed in the preceding section, and I_o. (E/I_o) decreases as the velocity spread increases, due to waveform distortion. But in general, as the velocity spread increases, I_o will increase too, making it necessary to analyze in more detail the behavior of their product, $(E/I_o)I_o$. If we assume that the atomic beam is shot-noise limited, the noise level within the measurement bandwidth will be proportional to $I_o^{1/2}$, so that the clock's signal-to-noise ratio will be proportional to $(E/I_o)I_o^{1/2}$.

Let $\phi(v)$ be the atomic beam intensity per unit speed interval before velocity selection within the tube of trajectories leading to the ionizer. If the speed distribution of the cesium atoms is beam-Maxwellian,

$$\phi(v) = \frac{2\phi_o}{\alpha}\left(\frac{v}{\alpha}\right)^3 \exp\left[-(v/\alpha)^2\right], \qquad (12)$$

where $\alpha = (2kT/m)^{1/2}$ and ϕ_o is the atomic beam intensity within the tube of trajectories leading to the ionizer prior to velocity selection. I_o is the corresponding intensity after velocity selection. Assuming unit transmission at the transmitted peak of the velocity distribution, $v = v_o$, it follows that $\phi(v_o)\, dv = I_o\, g(v_o)dv$, which results in $I_o = \phi(v_o)/g(v_o)$. For our choice of a Gaussian velocity distribution, $v_o = \bar{v}$ and

$$I_o = \sqrt{8\pi}\, \phi_o\, \frac{\sigma}{\alpha} \left(\frac{\bar{v}}{\alpha}\right)^3 \exp\left[-(\bar{v}/\alpha)^2\right]. \qquad (13)$$

Eq. 13 shows that for a given oven temperature and fixed average speed $\bar{v}$, I_o will be proportional to the Gaussian's standard deviation σ. The error signal will be proportional to $(E/I_o)\,\sigma$, and the signal-to-noise ratio will be proportional to $(E/I_o)\,\sigma^{1/2}$.

The results shown in Fig. 6 were obtained using the same set of parameters used before, and illustrate the results of the two competing effects described in this section. For relatively narrow speed distributions (up to $\sigma \tilde{=} 18$ m/s in our test case), intensity effects are dominant and the signal increases quasi-linearly with increasing velocity spread. As the speed distribution becomes broader, waveform distortion effects become dominant. The signal-to-noise ratio shows a maximum at $\sigma \tilde{=} 18$ m/s and then decreases slowly with increasing σ when waveform distortion effects become dominant.

V. CONCLUSIONS

The distribution of atomic arrival times at the cesium beam tube ionizer, as well as the distribution of ionic residence times on the ionizer, affect the performance of a cesium beam tube by distorting the time-dependence of the cesium ion current relative to the amplitude modulation impressed on the state-selected atomic beam by the combination of microwave interrogation and state analysis. This distortion results in a reduction of the error signal relative to the average ion current, and thus leads to degradation of the clock's discriminator function.

Figure 7 presents the frequency response of the post-microwave segment of a cesium beam tube for $\varepsilon = 1$, $d = 1$, $\bar{v} = 114$ m/s and $t_A = 1.4 \times 10^{-3}$ s. For a single-velocity beam and prompt ionization ($\tau = 0$), $|E|/I_o = 1/2$, independent of modulation frequency, as illustrated by the dotted line. If now the ionizer exponential distribution of residence times is incorporated, Eqs. 2 and 7a, b, combined with $\langle I_+ \rangle = I_o/2$, yield

$$\frac{|E|}{I_o} = \frac{1}{2} - 2\nu_m t^* + 2\nu_m \tau \left[1 - 2\,\Xi \exp\left(-t^*/\tau\right)\right] \qquad (14)$$

where $t^* = \tau\, \ell n\, (2\,\Xi)$. This result is indicated by the dash line. The solid line shows the effect of replacing the single-velocity atomic beam by one having a Gaussian distribution of $\sigma = 10$ m/s. In this particular case, the main effect of the velocity spread in the atomic beam is to force a much sharper signal cut-off as the modulation frequency increases.

In light of these results, our main conclusion is that when determining the frequency modulation scheme, attention should be paid not only to the atomic interaction with the microwave field in the Ramsey cavities, but also

these "post-microwave segment" effects. Waveform distortion effects can be minimized by choosing an appropriate operating point on the frequency response curve of the "post-microwave segment" of the cesium beam tube.

ACKNOWLEDGMENTS

I would like to thank Drs. R. Frueholz and S. Karuza and Mr. W. Johnson for some illuminating discussions. This work was supported by the United States Air Force Space Division under Contract No FO4701-85-CC-0086.

REFERENCES

[1] F. L. Hughes and H. Levinstein, "Mean adsorption lifetime of Rb on etched tungsten single crystals: ions," Phys. Rev., vol. 113, pp. 1029-1035, 1958.

[2] E. G. Nazarov, "Observation of atomic desorption dynamics with a voltage-modulation method," Sov. Phys. Tech. Phys. vol. 24, pp. 707-710, 1979. (Transl. from Zh. Tekh. Fiz. vol. 49, pp. 1277-1281, 1979).

[3] C. Audoin, V. Candelier and J. Vanier, "Effect of the atom transit time on the frequence stability of cesium beam frequency standards," Proc. 40th Ann. Freq. Control Symposium. New York: IEEE 1986, pp. 432-440.

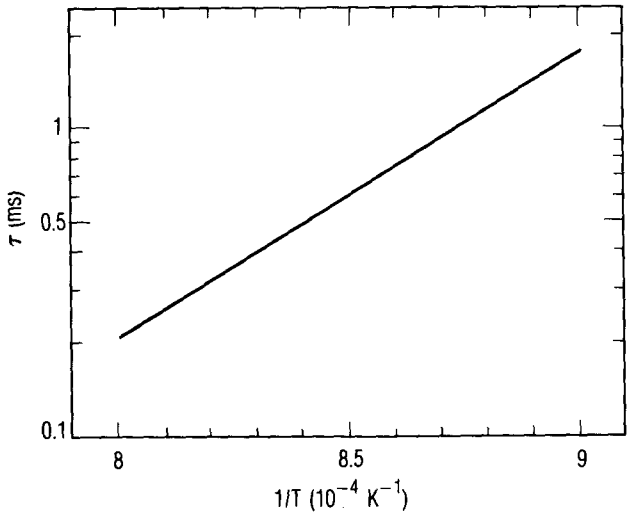

Fig. 1 Cesium ion dwell time vs. tungsten wire inverse absolute temperature from Nazarov [2].

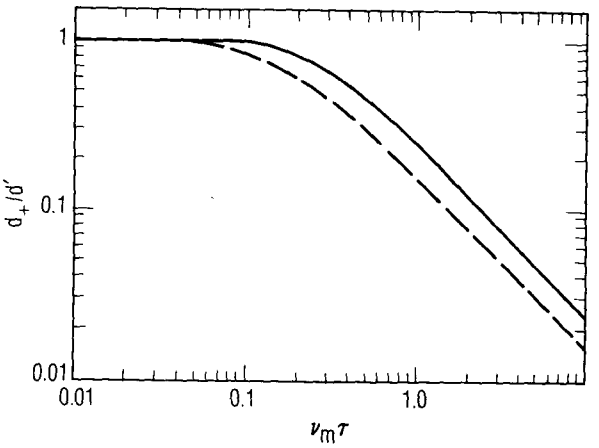

Fig. 2 Response of ionizer to an amplitude-modulated atomic beam. Abscissa: modulation frequency times ionic dwell-time. Ordinate: ratio of ion current to atomic current modulation depths. Solid line: square wave modulation. Dash line: sine wave modulation.

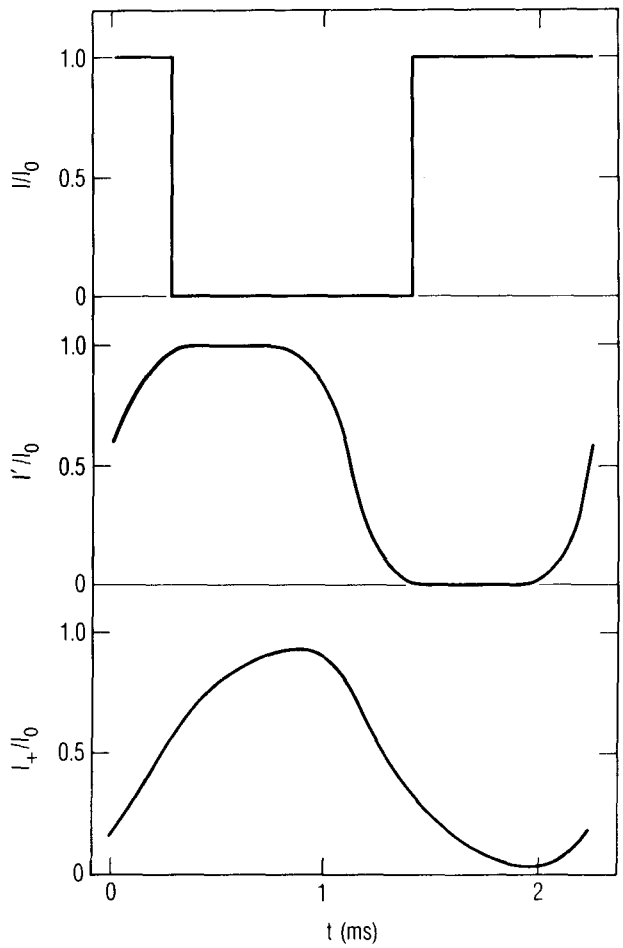

Fig. 3 Amplitude-modulated waveforms. Top: atomic beam square-wave modulation. Middle: atomic beam incident on ionizer. Bottom: ion current. $\bar{v}$ = 114 m/s, σ = 10 m/s, $\bar{t}_A = 1.4 \times 10^{-3}$ s, ν_m = 440 Hz, $\tau = 3 \times 10^{-4}$ s, d = 1, ϵ = 1.

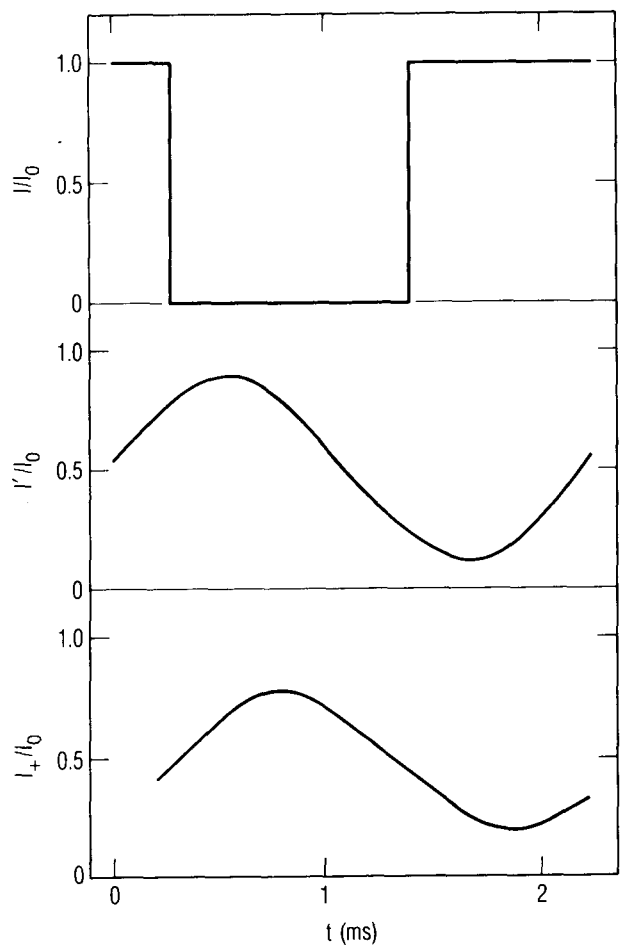

Fig. 4 Amplitude-modulated waveform. Top: atomic beam square-wave modulation. Middle: atomic beam incident on ionizer. Bottom: ion current. $\bar{v}$ = 114 m/s, σ = 30 m/s, $\bar{t}_A = 1.4 \times 10^{-3}$ s, ν_m = 440 Hz, $\tau = 3 \times 10^{-4}$ s, d = 1, ϵ = 1.

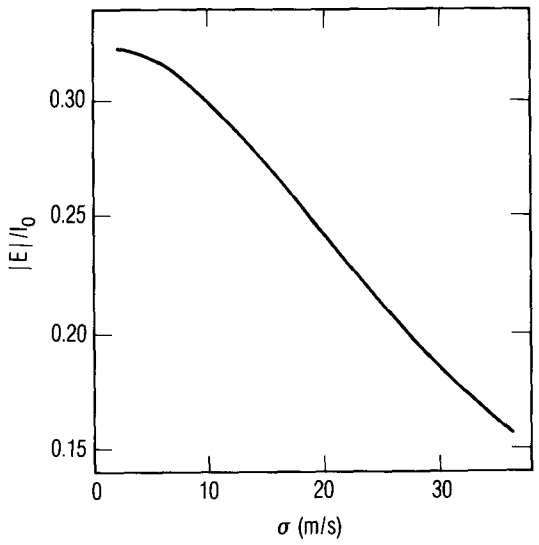

Fig. 5 Relative error signal vs. velocity distribution width. $\bar{v}$ = 114 m/s, $\bar{t}_A = 1.4 \times 10^{-3}$ s, ν_m = 440 Hz, $\tau = 3 \times 10^{-4}$ s, d = 1, $\epsilon = 1$.

Fig. 6 Signal (top) and signal-to-noise ratio (bottom) (arbitrary units) vs. velocity distribution width. $\bar{v}$ = 114 m/s, $\bar{t}_A = 1.4 \times 10^{-3}$ s, ν_m = 440 Hz, $\tau = 3 \times 10^{-4}$ s, d = 1, $\epsilon = 1$.

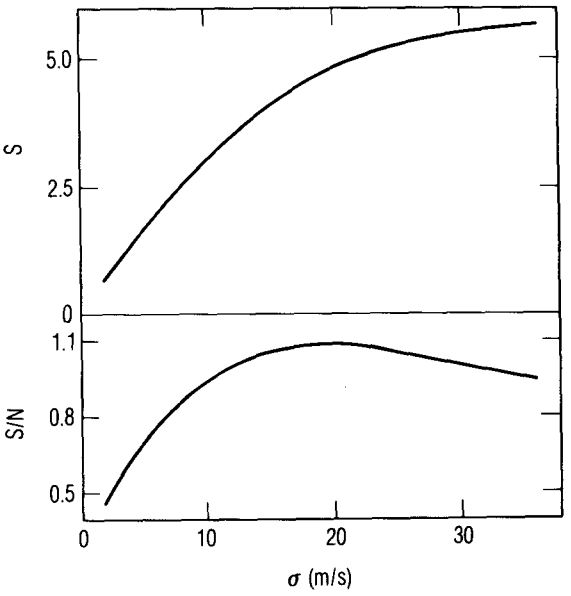

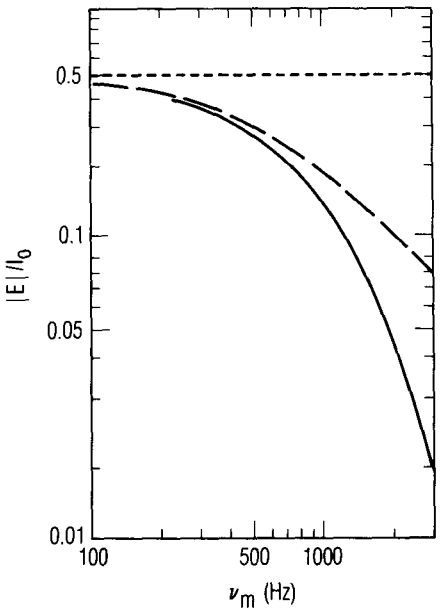

Fig. 7 Relative error signal vs. modulation frequency. $\bar{v}$ = 114 m/s, $\bar{t}_A = 1.4 \times 10^{-3}$ s, d = 1, $\epsilon = 1$. Dotted line: no distortion. Dash line: single-velocity beam, $\tau = 3 \times 10^{-4}$ s. Solid line: σ = 10 m/s, $\tau = 3 \times 10^{-4}$ s.

David Allan, National Bureau of Standards: Have you applied your theory to the different kinds of tubes that are available to us?

Mr. Jaduszliwer: That is the next step. I would like now to examine some realistic modulation schemes and see what happens.

Len Cutler, Hewlett Packard: (Gave a comment which was not into the microphone and not intelligible.)